Contrib Mineral Petrol (2002) 143: 56–70
DOI 10.1007/s00410-001-0331-8

Sonja Aulbach · Thomas Stachel · K. Stephanus Viljoen
Gerhard P. Brey · Jeff W. Harris

Eclogitic and websteritic diamond sources beneath the Limpopo Belt – is slab-melting the link?

Received: 4 October 2000 / Accepted: 31 October 2001 / Published online: 12 January 2002

Abstract Trace-element concentrations in eclogitic and websteritic inclusions in diamonds from Venetia (South Africa) were analysed using an ion microprobe (SIMS). Garnets of both parageneses show similar, positive $LREE_N/HREE_N$ slopes, but eclogitic garnets have higher MREE and almost flat $MREE_N$–$HREE_N$, and are also different in having significantly higher Sr and Zr. The occurrence of negative and positive Eu anomalies in garnets and clinopyroxenes of both parageneses points towards feldspar fractionation and accumulation in a magmatic precursor, suggesting subducted oceanic crust as a common protolith. Assuming equilibrium between clinopyroxene and garnet included in the same diamond, a bulk eclogite was reconstructed from these inclusions plus (expected) accessory rutile. The whole rock has a trace-element pattern lying between oceanic gabbro and EMORB, but is depleted in highly incompatible elements relative to these possible precursors. Quantitative modelling shows that relative and absolute trace-element abundances of the reconstructed eclogite and the hypothetical oceanic precursor agree if the latter is subjected to a loss of partial melts after subduction into the eclogite stability field. Major- and trace-element characteristics of websteritic inclusions could imply a more mafic precursor, which may have been part of a heterogeneous oceanic crust. However, new experimental data show that major- and trace-element compositions of websteritic inclusions in diamond are consistent with a mixing model in which they result from the reaction of slab-derived melts with surrounding mantle peridotite. This reaction generates major element contents that are intermediate between those of eclogitic and peridotitic sources whereas trace-element characteristics, such as Eu anomalies, are inherited from the melt source.

S. Aulbach (✉) · T. Stachel · G.P. Brey
Institut für Mineralogie, Universität Frankfurt,
Senckenberganlage 28, 60054 Frankfurt, Germany
E-mail: saulb001@laurel.ocs.mq.edu.au

K.S. Viljoen
GeoScience Centre, De Beers Consolidated Mines Ltd,
P.O. Box 82232, Southdale 2135, South Africa

J.W. Harris
Division of Earth Sciences, University of Glasgow,
Glasgow G12 8QQ, Scotland, UK

Present address: S. Aulbach
GEMOC ARC National Key Centre,
Macquarie University, NSW 2109, Australia

Present address: T. Stachel
Department of Earth and Atmospheric Sciences,
University of Alberta, T6G 2E3, Canada

Editorial responsibility: J. Hoefs

Introduction

Diamonds and their inclusions are valuable for mantle research because they represent samples that, unlike xenoliths, are unadulterated by reactions with the transporting magma or by later alteration processes. Two main inclusion suites (peridotitic and eclogitic) with distinct assemblages and geochemical characteristics have long been recognised (Meyer and Boyd 1972; Sobolev 1977). In this contribution, we focus on a third paragenesis (websteritic inclusions) and its relationship to the eclogitic suite.

Researchers have long debated whether eclogites represent subducted former oceanic crust or whether they have crystallised from a primary mantle melt at depth. We discuss the arguments used by the different factions and present trace-element data and modelling to elucidate the origin of the eclogitic diamond source at Venetia.

Websteritic inclusions in diamonds are a rare and only little studied paragenesis, which is chemically transitional between the dominant eclogitic and peridotitic reservoirs (Gurney et al. 1984; Deines et al. 1993). We report here the first trace-element data for inclusions of this paragenesis and discuss current models for an igneous formation of websterites that are based on evidence from xenoliths and orogenic massifs. An

alternative model is presented that focuses on the intermediate major-element content and the trace-element characteristics of websteritic inclusions in diamond and that finds support in recent experimental works.

Samples and analytical methods

Mineral inclusions in 200 diamonds from the Venetia Mine were released by crushing after visual examination (Viljoen et al. 1999). Eclogitic inclusions were studied from 12 diamonds (19 garnets, two clinopyroxenes) and websteritic inclusions from nine diamonds (11 garnets, 13 clinopyroxenes, two orthopyroxenes), with one diamond containing a mixed paragenesis of three eclogitic garnets and a websteritic orthopyroxene. None of the inclusions used for the present study are in contact with another. With the exception of diamond v163, none of the diamonds were visibly cracked and, therefore, are assumed to represent unaltered samples of the diamondiferous mantle. These inclusions were carefully analysed by EPM to achieve high precision and low detection limits. Subsequently, five websteritic and five eclogitic garnets, and five websteritic and two eclogitic clinopyroxenes were selected as representative samples for ion probe analysis.

Major- and minor-element data were collected using the Jeol JXA-8900 RL electron microprobe at Frankfurt University. Counting times were chosen such that detection limits of 100 ppm or better were achieved for all oxides except Na_2O (~200 ppm). Acceleration voltage and probe current were set at 20 kV and 20 nA, respectively. Matrix corrections were carried out using algorithms of J.T. Armstrong implemented in the Jeol software.

Trace-element data were measured with the Cameca IMS 4f ion microprobe at Edinburgh University. Counts for each element and the background were collected for 50 s and corrections were made for isobaric interferences, e.g. BaO on Eu and ZrH on Nb. Element abundances were determined by calibrating the sensitivity for each element against SRM610 glass standard and using Si as an internal standard. Analytical conditions are described in more detail in Stachel and Harris (1997).

Inclusion chemistry

Major- and trace-element data are given in Tables 1 and 2. The reader is also referred to Viljoen et al. (1999) for a more extensive data set on the major-element composition of inclusions in diamonds from Venetia. The assignment of inclusions to a specific paragenesis, i.e. eclogitic, websteritic or peridotitic, could be unambiguously done on the basis of major element composition alone for all of the garnet and orthopyroxene inclusions, using the criteria outlined below. For clinopyroxene inclusions, where the websteritic paragenesis compositionally falls between, but also overlaps with the eclogitic and peridotitic paragenesis, a combination of clinopyroxene composition and the paragenesis of garnet occurring within the same diamond was used.

Major elements

Garnet

The distinction between peridotitic and eclogitic garnet inclusions may be made on the basis of the low Cr content of the latter (Gurney 1984; Meyer 1987), and we have used an arbitrary cut-off at 1 wt% Cr_2O_3 (Fig. 1). After the recognition of a websteritic inclusion paragenesis at Orapa, Deines et al. (1993) introduced a diagram Cr_2O_3 versus Mg-number to distinguish peridotitic, websteritic and eclogitic garnets. For Venetia, this classification scheme fails to correctly assign observed parageneses based on inclusion mineralogy and a new criterion had to be established. Here we use a plot of CaO versus Cr_2O_3 (Fig. 1), which is conventionally used to separate lherzolitic garnets formed in equilibrium with both clinopyroxene and orthopyroxene from wehrlitic (only in equilibrium with cpx) and harzburgitic (no clinopyroxene present in the source) garnets (Sobolev et al. 1973). Applying the 1 wt% Cr_2O_3 cut-off from the peridotitic suite, we used the same compositional fields to distinguish between eclogitic garnets in equilibrium with clinopyroxene only (i.e. eclogite sensu stricto) and websteritic garnets co-existing with both clinopyroxene and orthopyroxene (± olivine; Fig. 1). While we acknowledge (1) that this rather formalistic approach excludes some of the more Cr-rich websteritic garnets from Orapa and (2) that the Ca-content in an orthopyroxene-free paragenesis may still be low enough to crystallise garnet plotting into the 'lherzolite field', we find that all observed websteritic garnets (i.e. that occur with an opx inclusion in the same diamond) at Venetia are correctly assigned.

The pyrope-contents [$100*Mg/(Mg + Fe^t + Ca + Mn)$] of the parageneses determined according to the criteria described above do not overlap and range from 32.4 to 50.5 mol% for eclogitic garnets, 53.0–66.9 mol% for websteritic and 71.0–90.5 mol% for peridotitic garnets.

Clinopyroxene

Na and Cr contents distinguish peridotitic clinopyroxene with low jadeite and high Cr ('Cr-diopside') from eclogitic clinopyroxene with high Na and Al ('omphacite') content. All inclusions that compositionally fall between the eclogitic and peridotitic paragenesis occur with websteritic garnet and were accordingly assigned to the websteritic paragenesis. This procedure is contingent on equilibrium between minerals occurring within the same diamond, which is not always given (e.g. Sobolev et al. 1998).

Figure 2 shows that websteritic clinopyroxenes cluster around two different Mg-numbers, one coinciding with eclogitic values (Mg# ~80), the other being intermediate between peridotitic and eclogitic values (Mg# ~85).

Orthopyroxene

Websteritic orthopyroxene inclusions are distinct from peridotitic orthopyroxenes in their lower Mg-numbers

Table 1. Major-element analyses (wt%) and standard deviations of eclogitic (*e*) and websteritic (*w*) garnet (*gt*) and clinopyroxene (*cpx*), and websteritic orthopyroxene (*opx*) inclusions in diamond from Venetia. *ol* Olivine; *cor* corundum; *n* number of analyses

Mineral	gt	SD	gt	SD	opx	SD	gt	SD	gt	SD	gt	SD	opx	SD	cpx	SD
Sample	v53a	($n=4$)	v53b	($n=6$)	v53c	($n=6$)	v53e	($n=5$)	v54a	($n=4$)	v54b	($n=3$)	v54c	($n=5$)	v54d	($n=6$)
Suite	e		e		w		e		w		w		w		w	
Assemblage	3gt, opx		3gt, opx		3gt, opx		3gt, opx		2gt, 2cpx,opx		2gt, 2cpx,opx		2gt, 2cpx,opx		2gt, 2cpx,opx	
P_2O_5	0.06	0.01	0.05	0.01	≤ 0.01		0.05	0.01	0.02	0.00	≤ 0.01		≤ 0.01		≤ 0.01	
SiO_2	39.83	0.10	40.31	0.06	53.65	0.13	40.65	0.12	40.60	0.13	41.38	0.47	54.93	0.20	54.12	0.13
TiO_2	0.48	0.01	0.56	0.01	0.70	0.02	0.49	0.01	0.38	0.00	0.41	0.01	0.06	0.01	0.16	0.01
Al_2O_3	22.94	0.11	23.13	0.05	1.15	0.03	23.05	0.06	22.46	0.20	22.40	0.15	0.90	0.01	2.72	0.04
Cr_2O_3	0.02	0.01	0.02	0.01	0.14	0.01	0.01	0.01	0.61	0.01	0.64	0.01	0.06	0.01	0.24	0.01
FeO	11.45	0.06	11.66	0.05	15.00	0.09	11.24	0.10	15.27	0.04	14.58	0.05	12.49	0.06	8.28	0.08
MnO	0.20	0.01	0.20	0.01	0.34	0.01	0.19	0.01	0.39	0.01	0.36	0.01	0.19	0.01	0.19	0.01
NiO	0.02	0.00	0.02	0.01	0.05	0.01	0.02	0.01	≤ 0.01		≤ 0.01		0.11	0.01	0.07	0.01
MgO	10.63	0.04	11.45	0.02	26.90	0.09	10.89	0.03	16.48	0.09	17.33	0.28	28.55	0.09	17.26	0.20
CaO	14.06	0.05	12.97	0.03	1.93	0.02	13.84	0.07	3.88	0.02	3.84	0.02	1.19	0.01	14.07	0.21
Na_2O	0.20	0.01	0.22	0.01	0.05	0.01	0.20	0.01	0.08	0.01	0.08	0.01	0.27	0.02	1.60	0.04
K_2O	≤ 0.01		≤ 0.01		≤ 0.01		≤ 0.01		≤ 0.01		≤ 0.01		≤ 0.01		0.23	0.01
Total	99.86	0.23	100.57	0.08	99.92	0.14	100.63	0.30	100.17	0.26	101.04	0.84	98.78	0.22	98.94	0.26

Mineral	cpx	SD	gt	SD	gt	SD	gt	SD	gt	SD	cpx	SD	gt	SD	gt	SD
Sample	v54e	($n=6$)	v55	($n=4$)	v56 + 56b	($n=12$)	v57	($n=4$)	v59a	($n=6$)	v59b	($n=5$)	v60	($n=6$)	v61	($n=4$)
Suite	w		e		e		w		w		w		w		e	
Assemblage	2gt, 2cpx,opx		gt		gt		gt		gt, cpx		gt, cpx		gt		gt	
P_2O_5	≤ 0.01		0.04	0.01	0.04	0.01	0.04	0.00	0.02	0.01	≤ 0.01		0.03	0.01	0.07	0.02
SiO_2	54.66	0.23	39.70	0.40	40.33	0.26	41.20	0.19	41.69	0.39	54.57	0.23	40.19	0.36	40.61	0.37
TiO_2	0.14	0.02	0.56	0.02	0.41	0.02	0.57	0.01	0.21	0.01	0.08	0.00	0.39	0.01	0.51	0.01
Al_2O_3	2.45	0.35	22.57	0.22	22.63	0.21	22.63	0.20	22.32	0.24	2.50	0.02	22.33	0.18	22.39	0.40
Cr_2O_3	0.22	0.04	0.08	0.01	0.02	0.01	0.07	0.01	0.75	0.01	0.26	0.01	0.08	0.01	0.02	0.01
FeO	8.62	0.84	17.62	0.01	11.89	0.05	15.28	0.11	11.28	0.08	5.50	0.04	16.13	0.16	14.75	0.08
MnO	0.19	0.01	0.32	0.01	0.19	0.01	0.32	0.01	0.28	0.01	0.13	0.01	0.31	0.01	0.29	0.01
NiO	0.07	0.01	≤ 0.01		0.02	0.01	≤ 0.01		≤ 0.01		0.09	0.01	≤ 0.01		≤ 0.01	
MgO	18.78	2.24	11.92	0.17	11.64	0.10	15.96	0.11	19.26	0.27	18.27	0.14	14.58	0.16	9.78	0.09
CaO	13.22	2.27	7.14	0.05	12.37	0.26	4.92	0.02	4.29	0.03	16.26	0.09	5.14	0.03	12.69	0.09
Na_2O	1.48	0.29	0.19	0.01	0.16	0.01	0.19	0.00	0.05	0.00	1.24	0.03	0.19	0.01	0.23	0.01
K_2O	0.16	0.03	≤ 0.01		≤ 0.01		≤ 0.01		≤ 0.01		0.09	0.01	≤ 0.01		≤ 0.01	
Total	99.99	0.33	100.15	0.75	99.69	0.28	101.17	0.34	100.15	0.66	98.99	0.44	99.37	0.39	101.34	0.57

Mineral	gt	SD	cpx	SD	gt	SD	gt	SD	gt	SD	gt	SD	gt	SD	gt	SD
Sample	v97a	($n=4$)	v97b	($n=6$)	v133	($n=3$)	v156b + c	($n=11$)	v157a	($n=4$)	v158a	($n=4$)	v159a	($n=6$)	v159c	($n=3$)
Suite	w		w		e		e		e		e		w		w	
Assemblage	gt, cpx		gt, cpx		gt		gt		gt		gt		2gt, 4cpx		2gt, 4cpx	
P_2O_5	0.02	0.01	0.02	0.02	0.05	0.01	0.04	0.01	0.06	0.01	0.02	0.01	≤ 0.01		≤ 0.01	
SiO_2	41.37	0.06	54.07	0.51	40.38	0.10	41.08	0.10	40.89	0.12	39.85	0.19	41.35	0.07	41.85	0.39
TiO_2	0.47	0.01	0.19	0.01	0.16	0.01	0.43	0.01	0.73	0.01	0.22	0.00	0.23	0.01	0.23	0.01
Al_2O_3	21.95	0.11	2.23	0.07	22.97	0.04	22.89	0.12	22.61	0.12	22.96	0.17	21.97	0.03	21.54	0.40

Cr_2O_3	0.87	0.02	0.28	0.01	0.07	0.01	0.20	0.01	0.08	0.01	0.07	0.01	0.85	0.01	0.86	0.01
FeO	15.36	0.23	8.94	0.11	7.51	0.02	9.58	0.05	12.21	0.04	11.24	0.10	11.21	0.12	11.33	0.06
MnO	0.41	0.01	0.22	0.01	0.15	0.01	0.21	0.01	0.23	0.02	0.18	0.01	0.30	0.01	0.30	0.00
NiO	≤ 0.01		0.06	0.01	≤ 0.01		0.02	0.01	≤ 0.01		≤ 0.01		≤ 0.01		0.02	0.01
MgO	16.49	0.08	17.40	0.31	11.98	0.01	13.88	0.05	9.40	0.05	8.99	0.09	18.75	0.04	19.37	0.19
CaO	3.92	0.04	14.71	0.23	15.59	0.06	11.31	0.05	14.44	0.08	16.07	0.08	4.20	0.02	4.23	0.04
Na_2O	0.07	0.01	1.40	0.02	0.11	0.01	0.17	0.01	0.25	0.02	0.13	0.00	0.04	0.01	0.04	0.01
K_2O	≤ 0.01		0.18	0.01	≤ 0.01		≤ 0.01		≤ 0.01		≤ 0.01		≤ 0.01		≤ 0.01	
Total	100.95	0.46	99.69	0.70	98.99	0.11	99.81	0.25	100.90	0.28	99.73	0.31	98.91	0.19	99.75	0.39
Mineral	cpx		cpx		cpx		gt		gt		cpx		opx		cpx	
Sample	v159d		v159e		v160a		v160b		v163a		v163e		v163f + g		v163h	
Suite	w	SD	w	SD	e	SD	e	SD	w	SD	w	SD	w	SD	w	SD
Assemblage	2gt, 4cpx	($n=3$)	2gt, 4cpx	($n=5$)	gt, cpx	($n=4$)	gt, cpx	($n=6$)	gt, ol, 2opx, 3cpx	($n=4$)	gt, ol, 2opx, 3cpx	($n=2$)	gt, ol, 2opx, 3cpx	($n=11$)	gt, ol, 2opx, 3cpx	($n=6$)
P_2O_5	≤ 0.01		≤ 0.01		≤ 0.01		0.02	0.01	≤ 0.01		≤ 0.01		≤ 0.01		≤ 0.01	
SiO_2	54.00	0.05	55.10	0.30	54.05	0.35	40.87	0.05	40.58	0.08	53.68	0.08	55.50	0.49	54.48	0.11
TiO_2	0.08	0.01	0.08	0.01	0.30	0.00	0.45	0.02	0.33	0.01	0.12	0.00	0.05	0.01	0.11	0.01
Al_2O_3	2.05	0.02	1.99	0.02	8.59	0.08	22.57	0.05	21.99	0.04	2.84	0.01	0.92	0.01	2.67	0.01
Cr_2O_3	0.24	0.01	0.25	0.01	0.07	0.01	0.11	0.01	0.67	0.01	0.38	0.01	0.08	0.01	0.25	0.01
FeO	5.92	0.07	5.94	0.03	4.96	0.04	13.76	0.09	14.01	0.06	8.25	0.06	12.10	0.10	7.92	0.09
MnO	0.16	0.00	0.15	0.01	0.08	0.01	0.32	0.01	0.33	0.01	0.19	0.02	0.17	0.01	0.18	0.01
NiO	0.08	0.00	0.07	0.01	0.03	0.01	≤ 0.01		≤ 0.01		0.07	0.00	0.11	0.00	0.07	0.01
MgO	18.55	0.04	18.35	0.17	11.34	0.11	13.01	0.08	17.26	0.11	17.35	0.01	29.47	0.35	17.73	0.11
CaO	16.57	0.05	16.26	0.07	15.14	0.08	9.31	0.03	3.75	0.03	13.80	0.10	1.17	0.01	14.34	0.07
Na_2O	0.91	0.01	0.87	0.03	4.32	0.07	0.18	0.01	0.07	0.01	1.90	0.04	0.31	0.01	1.75	0.03
K_2O	0.09	0.01	0.09	0.01	0.08	0.01	≤ 0.01		≤ 0.01		0.14	0.00	≤ 0.01		0.19	0.01
Total	98.65	0.14	99.16	0.55	98.98	0.25	100.61	0.19	99.00	0.23	98.72	0.18	99.90	0.91	99.69	0.35
Mineral	gt		cpx		cpx		cpx		cpx		gt		gt		gt	
Sample	v166abc		v166d		v166e		v166f		v166g		v176a		v176b		v176c	
Suite	w	SD	w	SD	w	SD	w	SD	w	SD	e	SD	e	SD	e	SD
Assemblage	gt, 4cpx	($n=15$)	gt, 4cpx	($n=4$)	gt, 4cpx	($n=6$)	gt, 4cpx	($n=9$)	gt, 4cpx	($n=6$)	3gt, cpx, cor	($n=2$)	3gt, cpx, cor	($n=5$)	3gt, cpx, cor	($n=6$)
P_2O_5	≤ 0.01		≤ 0.01		≤ 0.01		≤ 0.01		≤ 0.01		0.04	0.01	0.04	0.02	0.03	0.01
SiO_2	41.42	0.41	54.20	0.10	54.42	0.16	54.12	0.19	54.80	0.10	39.75	0.07	39.90	0.22	40.35	0.21
TiO_2	0.32	0.01	0.16	0.00	0.16	0.01	0.16	0.01	0.16	0.00	0.10	0.00	0.10	0.01	0.10	0.01
Al_2O_3	22.48	0.18	3.69	0.03	3.92	0.02	3.85	0.04	4.05	0.02	22.95	0.06	22.99	0.04	22.46	0.07
Cr_2O_3	0.28	0.01	0.14	0.01	0.12	0.01	0.13	0.01	0.13	0.01	0.04	0.01	0.04	0.00	0.02	0.01
FeO	14.10	0.06	7.00	0.04	7.14	0.06	7.09	0.05	7.00	0.04	10.35	0.10	10.35	0.05	10.44	0.06
MnO	0.29	0.01	0.13	0.01	0.13	0.01	0.13	0.01	0.14	0.01	0.24	0.01	0.23	0.01	0.23	0.01
NiO	0.02	0.01	0.08	0.01	0.07	0.01	0.07	0.01	0.08	0.01	≤ 0.01		≤ 0.01		≤ 0.01	
MgO	17.04	0.21	16.21	0.04	16.25	0.05	16.21	0.04	16.48	0.03	10.08	0.04	10.18	0.07	8.84	0.09
CaO	4.60	0.04	15.10	0.05	14.88	0.02	14.81	0.04	14.67	0.06	15.50	0.05	15.44	0.10	16.76	0.15
Na_2O	0.10	0.01	2.11	0.01	2.16	0.04	2.12	0.04	2.21	0.04	0.10	0.01	0.11	0.01	0.10	0.01
K_2O	≤ 0.01		≤ 0.01		≤ 0.01		≤ 0.01		≤ 0.01		≤ 0.01		≤ 0.01		≤ 0.01	
Total	100.65	0.61	98.80	0.26	99.27	0.27	98.70	0.36	99.72	0.20	99.15	0.06	99.38	0.22	99.35	0.38

Table 1. (Contd.)

Mineral	cpx		gt		gt		gt		gt		gt		cpx	
Sample	v176d		v178ab		v180a		v180b		v180c		v181b		v199a		v199b	
Suite	e	SD	e	SD	e	SD	e	SD	e	SD	e	SD	w	SD	w	SD
Assemblage	3gt, cpx, cor	($n=3$)	gt	($n=12$)	3gt	($n=5$)	3gt	($n=6$)	3gt	($n=5$)	gt	($n=5$)	gt, cpx	($n=3$)	gt, cpx	($n=3$)
P_2O_5	≤ 0.01		0.10	0.01	0.07	0.01	0.06	0.01	0.06	0.02	0.03	0.01	≤ 0.01		≤ 0.01	
SiO_2	51.37	0.12	40.16	0.25	39.48	0.32	39.75	0.25	39.21	0.08	40.42	0.17	40.95	0.07	54.52	0.22
TiO_2	0.05	0.01	0.69	0.01	0.79	0.01	0.77	0.01	0.80	0.01	0.30	0.01	0.36	0.02	0.16	0.00
Al_2O_3	21.26	0.04	22.26	0.19	22.36	0.05	22.55	0.06	21.93	0.06	23.07	0.08	21.50	0.07	2.62	0.03
Cr_2O_3	0.03	0.01	0.07	0.01	0.02	0.01	0.03	0.01	0.02	0.01	0.04	0.01	0.66	0.00	0.24	0.01
FeO	2.10	0.02	17.85	0.18	12.51	0.03	12.61	0.09	12.42	0.04	12.01	0.05	14.52	0.09	8.14	0.04
MnO	0.03	0.01	0.32	0.01	0.20	0.01	0.21	0.01	0.21	0.01	0.20	0.01	0.35	0.00	0.19	0.00
NiO	0.03	0.01	≤ 0.01		≤ 0.01		0.01	0.00	≤ 0.01		≤ 0.01		≤ 0.01		0.07	0.00
MgO	4.80	0.01	11.00	0.14	8.66	0.10	8.83	0.05	8.62	0.05	11.03	0.14	17.35	0.04	16.96	0.13
CaO	10.61	0.03	8.14	0.08	15.19	0.06	15.21	0.07	15.19	0.04	12.94	0.06	3.59	0.01	14.15	0.03
Na_2O	8.40	0.06	0.25	0.01	0.27	0.01	0.28	0.01	0.27	0.01	0.13	0.01	0.07	0.00	1.54	0.03
K_2O	0.05	0.00	≤ 0.01		≤ 0.01		≤ 0.01		≤ 0.01		≤ 0.01		≤ 0.01		0.19	0.01
Total	98.72	0.09	100.85	0.53	99.57	0.43	100.30	0.21	98.73	0.05	100.19	0.45	99.36	0.20	98.80	0.39

(76.2–81.3; peridotitic: 90.2–94.9) and higher CaO (1.2–1.9 wt%; peridotitic: 0.1–1.0 wt%) and TiO_2 contents (0.05–0.7 wt%; peridotitic: <0.01–0.05 wt%). They also tend to have lower Cr_2O_3 and higher Na_2O. Following the criterion set by Deines et al. (1993), orthopyroxene inclusions with Mg-numbers <88 were assigned to the websteritic paragenesis, those with Mg-number >88 to the peridotitic suite.

Trace elements

The eclogitic suite

Eclogitic garnets from Venetia have a steep positive slope in $LREE_N$ and flat $MREE_N$ and $HREE_N$ at five to ten times chondritic abundance (Fig. 3a), except for v176c and v160b. Similar REE patterns were observed in eclogitic inclusions in diamonds from Udachnaya, Mir and Mwadui (Ireland et al. 1994; Taylor et al. 1996; Stachel et al. 1998, 1999).

The REE pattern for v176c differs markedly from that of other eclogitic garnets in that it has superchondritic LREE and a trough in the MREE together with a positive Eu-anomaly. This inclusion also has 16.8 wt% CaO, the highest for all Venetia garnets and occurs with corundum (Viljoen et al. 1999). Garnet v160b is distinctive in view of the high Pr, Nd, and Sm, but particularly because of the marked positive Eu anomaly (see Fig. 3a). Concentrations of LIL (large-ion-lithophile) and HFS (high-field-strength) elements of all the eclogitic garnets (Fig. 3b) increase from Ba_N to Ti_N, remain constant at about five times chondritic for Ti, Zr and Hf and then increase slightly for Y_N.

The REE_N patterns for the two eclogitic clinopyroxenes are shown in Fig. 4a. Both occur with garnet in the same diamond, but have quite different REE patterns. V176d has La, Ce and Pr abundances six to nine times chondritic and subchondritic values for Sm, with other MREE and HREE at 0.1 to 0.3 chondritic abundance and non-detectable Lu. The REE concentrations of v160a rise from $La_N = 3$ to $Nd_N = 20$ before decreasing to sub-chondritic Lu_N concentrations. Like the garnet occurring in the same diamond, v160a has a distinct positive Eu anomaly. Figure 4b shows that v160a is also characterised by an extremely high Sr content and that v176d has low Ba, Zr, Hf and Y.

The websteritic suite

REE_N of websteritic garnets form a narrow band with a positive $LREE_N/HREE_N$ slope (Fig. 3a), except for La_N/Ce_N where three garnets have a ratio >1. Two garnets show small negative Eu anomalies, whereas the two garnets with $La_N/Ce_N < 1$ show small positive Eu anomalies. The range of Ba, Nb, Ti, Hf and Y (Fig. 3b) concentrations is similar to that of eclogitic garnets, Sr is significantly depleted and Zr is fairly low relative to

Table 2. Trace-element analyses of selected garnet and clinopyroxene inclusions listed in Table 1. Abbreviations as in Table 1. *n.d.* Not detected; unit is (ppm)

Mineral	gt	gt	gt	cpx	gt	cpx	gt	cpx	gt		cpx	gt		cpx	gt	cpx
Sample	v55	v56	v59a	v59b	v97a	v97b	v156b	v160a	v160b	v163a	v163e	v166c	v166f	v176c	v176d	v199a	v199b
Suite	e	e	w	w	w	w	e	e	e	w	w	w	w	e	e	w	w
Assemblage	gt	gt	gt, cpx	gt, cpx	gt, cpx	gt, cpx	gt	gt, cpx	gt, cpx	gt, ol, opx, cpx	gt, ol, opx, cpx	gt, cpx	gt, cpx	gt, cpx, cor	gt, cpx, cor	gt, cpx	gt, cpx
Ti	2,820.00	1,910.00	1,000.00	408.00	2,460.00	1,060.00	2,170.00	1,510.00	2,390.00	1,610.00	631.00	1,500.00	806.00	493.00	219.00	1,820.00	807.00
Sr	1.13	1.23	0.19	35.00	0.16	12.30	1.70	556.00	8.77	0.11	8.67	0.58	98.80	4.62	50.00	0.13	13.80
Y	25.70	9.94	6.73	0.95	19.00	3.66	6.36	0.60	9.47	13.80	2.35	13.70	2.25	17.40	0.16	18.10	3.37
Zr	16.10	14.50	4.49	1.03	4.78	0.68	24.20	8.93	23.40	3.72	0.67	6.79	2.10	3.32	0.12	4.17	1.12
Nb	0.09	0.43	0.14	0.14	0.32	0.20	0.69	0.47	0.34	0.65	1.07	0.06	0.08	3.27	0.79	1.39	0.57
Ba	0.04	0.12	0.04	0.28	0.02	3.32	0.02	0.58	0.01	0.06	26.20	0.04	95.00	0.03	0.04	0.02	4.39
La	0.03	0.06	0.01	0.34	0.03	1.32	0.05	0.84	0.04	0.08	3.64	0.01	0.62	2.27	1.54	0.08	2.99
Ce	0.21	0.41	0.06	1.04	0.19	3.31	0.46	3.58	0.46	0.13	1.61	0.06	1.53	14.60	5.45	0.05	3.05
Pr	0.06	0.13	0.02	0.15	0.04	0.22	0.16	1.23	0.33	0.02	0.10	0.02	0.24	2.22	0.52	0.01	0.21
Nd	0.80	1.39	0.13	0.72	0.23	0.98	1.69	10.40	5.82	0.13	0.73	0.26	1.77	7.15	0.93	0.25	1.41
Sm	0.71	0.92	0.17	0.18	0.27	0.53	0.93	0.87	1.63	0.24	0.43	0.37	0.54	0.76	0.05	0.34	0.70
Eu	0.53	0.44	0.11	0.10	0.17	0.19	0.41	0.51	1.29	0.13	0.10	0.24	0.01	0.43	0.02	0.18	0.29
Gd	2.40	1.78	0.45	0.27	1.05	0.82	1.57	0.59	1.55	0.96	0.58	0.98	0.81	0.83	0.07	1.16	1.05
Tb	0.59	0.34	0.11	0.06	0.28	0.14	0.20	0.03	0.27	0.21	0.07	0.26	0.11	0.26	0.01	0.31	0.16
Dy	4.53	2.16	0.99	0.30	2.75	0.94	1.47	0.30	2.00	2.15	0.52	2.23	0.73	2.94	0.05	2.76	0.88
Ho	1.09	0.47	0.29	0.04	0.82	0.15	0.29	0.04	0.44	0.60	0.11	0.56	0.12	0.81	0.01	0.78	0.18
Er	3.62	1.01	0.97	0.13	3.20	0.47	0.70	0.06	1.31	2.03	0.42	2.06	0.29	2.54	0.04	2.92	0.42
Yb	3.72	0.82	1.39	n.d.	5.10	n.d.	0.67	n.d.	1.51	2.71	n.d.	2.41	n.d.	2.56	n.d.	3.81	n.d.
Lu	0.70	0.13	0.21	0.01	1.03	0.08	0.11	0.01	0.22	0.48	0.06	0.38	0.02	0.32	<0.005	0.70	0.04
Hf	0.41	0.27	0.10	0.06	0.30	0.12	0.50	0.47	0.53	0.30	0.14	0.37	0.25	0.04	0.02	0.47	0.17

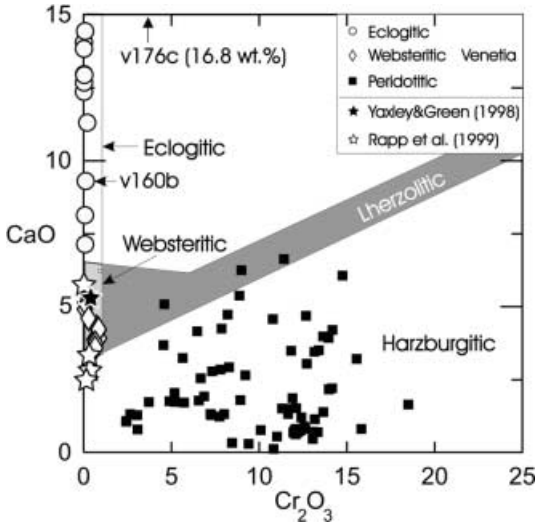

Fig. 1. Garnet inclusions in diamond from Venetia: CaO versus Cr_2O_3 (wt%) with lherzolitic and harzburgitic fields after Sobolev et al. (1973). Experimental run products of Yaxley and Green (1998) and of Rapp et al. (1999), which are referred to in the discussion, are also shown. A value of 1 wt% Cr_2O_3 was chosen to separate the websteritic field from the lherzolitic trend

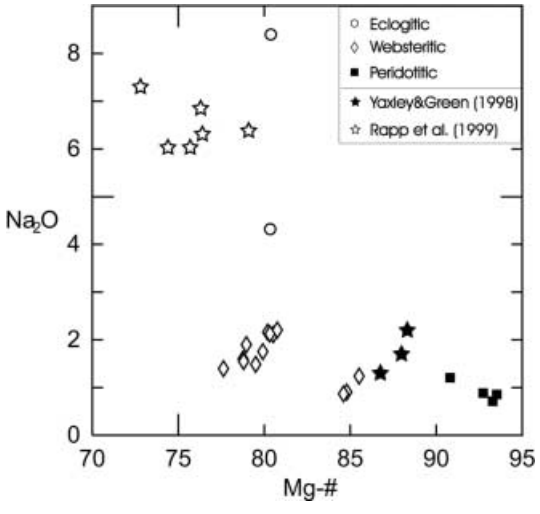

Fig. 2. Clinopyroxene inclusions in diamond from Venetia. Diagram of Mg# versus log Na_20. Experimental data as in Fig. 1

the eclogitic suite. With one exception (v166f), the REE_N patterns of the clinopyroxenes, shown in Fig. 4a, are almost flat, peaking at Eu or Gd. Three clinopyroxenes show negative slopes from La to Pr (cf. the garnet patterns in Fig. 3a). Negative Eu anomalies are displayed by two clinopyroxenes, a positive Eu anomaly by one clinopyroxene. Clinopyroxene v166f, which has a pronounced negative anomaly (see Fig. 4a), occurs in the same diamond with a garnet with a small positive Eu anomaly, an observation that may indicate possible disequilibrium between the two inclusions. However, in contrast to garnet, two websteritic clinopyroxenes have significant Ba contents (95 ppm in the

Table 3. Trace-element partitioning between clinopyroxene (*cpx*) and garnet (*grt*) for websteritic and eclogitic inclusions from Venetia, the equation and constants determined empirically by Harte and Kirkley (1997) for an equilibrated eclogite suite from Roberts Victor, Rutile; *amp* amphibole; *n.a.* not available

Mineral	$D^{cpx/grt}$	Calc from	$D^{cpx/grt}$	Calc from	$D^{cpx/grt}$	Calc from	$D^{cpx/grt}$	Calc from	$D^{cpx/grt}$
Sample	v59	D_{Ca*}[a]	v97	D_{Ca*}[a]	v160	D_{Ca*}[a]	v163	D_{Ca*}[a]	v166
Suite	w		w		e		w		w
Assemblage	grt, cpx		grt, cpx		grt, cpx		grt, cpx		grt, cpx
Ca*	3.85		3.79		1.61		3.69		3.26
Ti	0.41	n.a.	0.43	n.a.	0.63	n.a.	0.39	n.a.	0.54
Sr	184.21	406.97	76.88	394.70	63.40	74.34	78.82	374.64	170.34
Y	0.14	0.14	0.19	0.14	0.06	0.03	0.17	0.13	0.16
Zr	0.23	0.86	0.14	0.85	0.38	0.50	0.18	0.83	0.31
Nb	1.00	n.a.	0.63	n.a.	1.38	n.a.	1.65	n.a.	1.33
Ba	7.00	2.31	166.00	2.28	58.00	0.97	436.67	2.22	2375.00
La	34.00	59.14	44.00	56.48	21.00	4.60	45.50	52.22	62.00
Ce	17.33	42.57	17.42	40.74	7.78	3.74	12.38	37.81	25.50
Pr	7.50	n.a.	5.50	n.a.	3.73	n.a.	5.00	n.a.	12.00
Nd	5.54	9.81	4.26	9.47	1.79	1.34	5.62	8.91	6.81
Sm	1.06	2.32	1.96	2.25	0.53	0.41	1.79	2.13	1.46
Eu	0.91	1.37	1.12	1.33	0.40	0.24	0.77	1.26	0.04
Gd	0.60	n.a.	0.78	n.a.	0.38	n.a.	0.60	n.a.	0.83
Tb	0.55	0.49	0.50	0.48	0.11	0.08	0.33	0.45	0.42
Dy	0.30	0.29	0.34	0.28	0.15	0.05	0.24	0.27	0.33
Ho	0.14	0.16	0.18	0.16	0.09	0.03	0.18	0.15	0.21
Er	0.13	0.11	0.15	0.11	0.05	0.03	0.21	0.10	0.14
Yb	n.a.	n.a.	n.a.	n.a.	n.a.	n.a.	n.a.	n.a.	n.a.
Lu	0.05	0.05	0.08	0.05	0.05	0.03	0.13	0.05	0.05
Hf	0.60	n.a.	0.40	n.a.	0.89	n.a.	0.47	n.a.	0.68

[a]Molar partition coefficient. Equation of Harte and Kirkley (1997)
[b]Experiment at 1,160 °C/40 kbar, Green et al. (2000)
[c]Average Kakanui pyroxenite, equilibration temperature 920 °C, Zack et al. (1997)

case of v166f; cf. Figs. 3b and 4b), which require large corrections for the isobaric interference of BaO on Eu. Therefore, contrary to the observations for garnets, the Eu anomalies found for websteritic clinopyroxenes may just be artefacts. All websteritic clinopyroxenes have near chondritic abundances of Ti, Hf and Y and a trough at Zr_N, but only three have a trough at Nb_N as well (Fig. 4b).

Clinopyroxene/garnet trace-element partitioning

Table 3 shows the partitioning of trace elements between garnet–clinopyroxene pairs ($D^{cpx/grt}$) from Venetia. In order to assess whether the inclusion assemblages are in equilibrium, we calculated the equilibrium partition coefficients based on the molar distribution of Ca ($D^{cpx/grt}_{Ca^*}$) between clinopyroxene and garnet (Table 3). We used the equation and empirically determined constants of Harte and Kirkley (1997), which are applicable for equilibration temperatures of $1{,}100 \pm 100$ °C at 50 kbar. Harte and Kirkley (1987) observed no co-variation of distribution coefficients with temperature across the temperature range of 947–1,285 °C for their eclogite suite, and the effect of diverging equilibration temperatures for inclusion pairs in diamond from Venetia is likely to be small.

Deviation from calculated equilibrium distribution for clinopyroxene and garnet in diamonds from Venetia was calculated as measured minus the calculated $D^{cpx/grt}$, and is shown in Fig. 5. The strongest deviations are observed for LILE and LREE, a moderate deviation for HFSE and MREE, and a weak deviation for HREE. This could indicate that the mineral pairs are not in equilibrium. Disequilibrium for Ba, Sr, La and Ce may be the result of incomplete equilibration with a LILE- and LREE-rich fluid immediately prior to entrapment of the inclusions. Some of the discrepancy between calculated and measured partitioning values may also be caused by differences in bulk composition other than Ca, and/or in equilibrium pressures and temperatures that are known to affect the distribution to varying degrees. However, a similar calculation for Kakanui garnet pyroxenite for which equilibrium has been demonstrated (Zack et al. 1997) and for equilibrated experiments on natural basanite by Green et al. (2000) reveals similar deviations to those of inclusions in diamond. This discrepancy may be caused by uncertainties in the correlations of LILE and LREE with Ca in the dataset of Harte and Kirkley (1997). These uncertainties may be related to late-stage alteration of xenolithic clinopyroxene (Harte and Kirkley 1997) and are amplified during calculation of $D^{cpx/grt}$ of LREE because these elements show the greatest change in distribution coefficient with bulk Ca.

Considering the similarity to experimental distribution coefficients, garnet and clinopyroxene in v160 appear to be in equilibrium despite their distinctive trace

determined from trace-element analyses. Partition coefficients were also calculated from molar partition coefficients for Ca (D_{Ca^*}) using South Africa. Experimental values for natural basanite (Green et al. 2000) and Kakanui pyroxenite (Zack et al. 1997) are also listed. *rt*

Calc from D_{Ca^*}[a]	$D^{cpx/grt}$ v176 e grt, cpx	Calc from D_{Ca^*}[a]	$D^{cpx/grt}$ v199 w grt, cpx	Calc from D_{Ca^*}[a]	$D^{cpx/grt}$ Run 1807[b] Basanite grt, cpx, rt	Calc from D_{Ca^*}[a]	$D^{cpx/grt}$ Kakanui[c] Pyroxenite grt, cpx ± amp	Calc from D_{Ca^*}[a]
	0.60		3.95		1.77		3.04	
n.a.	0.44	n.a.	0.44	n.a.	n.a.	n.a.	n.a.	n.a.
294.23	10.82	10.85	106.15	427.84	140.00	89.43	217.43	256.75
0.11	0.01	0.00	0.19	0.15	0.05	0.03	0.16	0.09
0.77	0.04	0.27	0.27	0.87	0.44	0.53	1.32	0.74
n.a.	0.24	n.a.	0.41	n.a.	n.a.	n.a.	201.25	n.a.
1.96	1.33	0.36	219.50	2.37	n.a.	1.06	n.a.	1.83
36.32	0.68	0.25	37.38	63.75	51.00	6.07	210.06	29.60
26.76	0.37	0.24	61.00	45.73	17.00	4.87	48.84	22.02
n.a.	0.23	n.a.	21.00	n.a.	7.90	n.a.	21.16	n.a.
6.71	0.13	0.14	5.64	10.40	4.00	1.67	9.55	5.73
1.67	0.07	0.06	2.06	2.44	n.a.	0.49	2.23	1.45
0.98	0.05	0.03	1.61	1.44	0.53	0.29	1.34	0.86
n.a.	0.08	n.a.	0.91	n.a.	0.34	n.a.	0.68	n.a.
0.35	0.04	0.01	0.52	0.52	0.16	0.10	0.43	0.30
0.21	0.02	0.01	0.32	0.31	0.11	0.06	0.28	0.18
0.12	0.01	0.01	0.23	0.17	0.07	0.04	n.a.	0.11
0.08	0.02	0.01	0.14	0.11	n.a.	0.03	0.12	0.07
n.a.	n.a.	n.a.	n.a.	n.a.	0.02	n.a.	0.04	n.a.
0.05	n.a.	0.01	0.06	0.05	n.a.	0.03	n.a.	0.04
n.a.	0.50	n.a.	0.36	n.a.	0.05	n.a.	3.12	n.a.

element patterns (see Figs. 3 and 4). The unusual trace element patterns observed for garnet and clinopyroxene in diamond v176 (Figs. 3 and 4) do not necessarily indicate disequilibrium between these phases, but can be partially explained in terms of their very low $D^{cpx/grt}_{Ca^*}$ (0.60). Still, deviations from experimental partitioning data and, additionally, significant differences in major-element composition of multiple garnets within the same diamond, suggest disequilibrium between some inclusion phases. Highly variable mineral compositions and disequilibrium between multiple eclogitic inclusions from the same diamond have been noted in many other studies (Sobolev et al. 1998; Taylor et al. 1998; Keller et al. 1999; Taylor et al. 2000). $D^{cpx/grt}$ for websteritic inclusions mostly agree with those of pyroxenites from Kakanui, but diverge for two mineral pairs, v163 and v166. In the case of v163, a crack to the surface of the host diamond was observed during visual inspection prior to crushing and the inclusion assemblage may have been altered after diamond formation.

The present data allow recognition of some bulk compositional effects on the distribution coefficient. However, because of the small sample number, these must be treated with caution. Eclogites, which have higher Na_2O and CaO and lower MgO contents than websterites, have higher $D^{cpx/grt}$ for Ti, Zr and Hf. $D^{cpx/grt}$ is higher for websterites for the remainder of the trace elements discussed here.

Eclogite whole-rock reconstruction

Assuming equilibrium between the mineral inclusions in diamond v160, which is supported by clinopyroxene/garnet trace-element partitioning values similar to calculated equilibrium $D^{cpx/grt}$ and to experimental data (Fig. 5), a bulk trace-element composition was calculated from garnet v160b, clinopyroxene v160a and rutile or ilmenite, respectively (referred to as 'bulk Venetia eclogite' or BVE in the following). Although not included in diamond v160, a Ti-phase has been identified in some eclogite xenoliths (e.g. Snyder et al. 1997; Barth et al. 2001) and studies on inclusions in diamond (e.g. Sobolev et al. 1997). Rutile or other Ti-phases have also been implied as a residual phase of slab melting because of Ti and Nb depletion in supra-subduction zone magmas (e.g. Ryerson and Watson 1987). A rutile-bearing eclogite reservoir has been postulated by Rudnick et al. (2000) based on the mass imbalance for Nb and Ta between continental crust and depleted mantle. An ilmenite composition in equilibrium with the garnet–clinopyroxene pair v160 has been calculated using the internally consistent set of distribution coefficients of Fujimaki et al. [(1984), $D^{ilm/melt}$ for Y from Nielsen et al. (1992) and for Eu from Paster and Schauwecker (1974)]. An average eclogitic rutile composition was taken from the literature (Sassi et al. 2000). We calculated a bulk rock with the mineral modes garnet:clinopyroxene:rutile

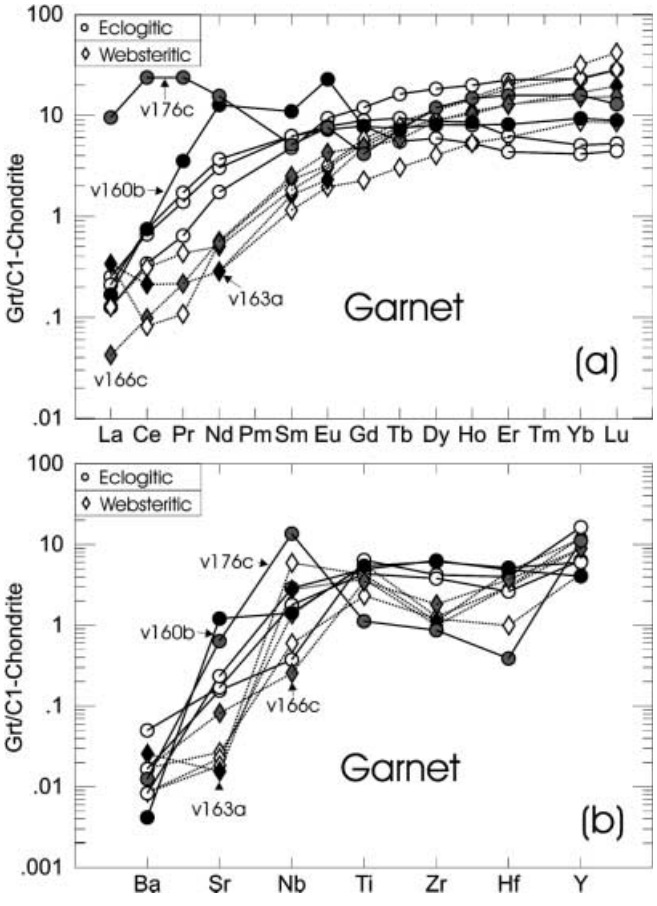

Fig. 3. **a** Garnet: REE-abundances. Note small positive and negative Eu anomalies in four of the five websteritic garnets. **b** LILE and HFSE-abundances; garnets v176c and v160b, which are referred to in the text, are indicated. V166c and v163a coexist with clinopyroxenes with distinct negative Eu anomalies. Normalised to C1-chondrite of McDonough and Sun (1995)

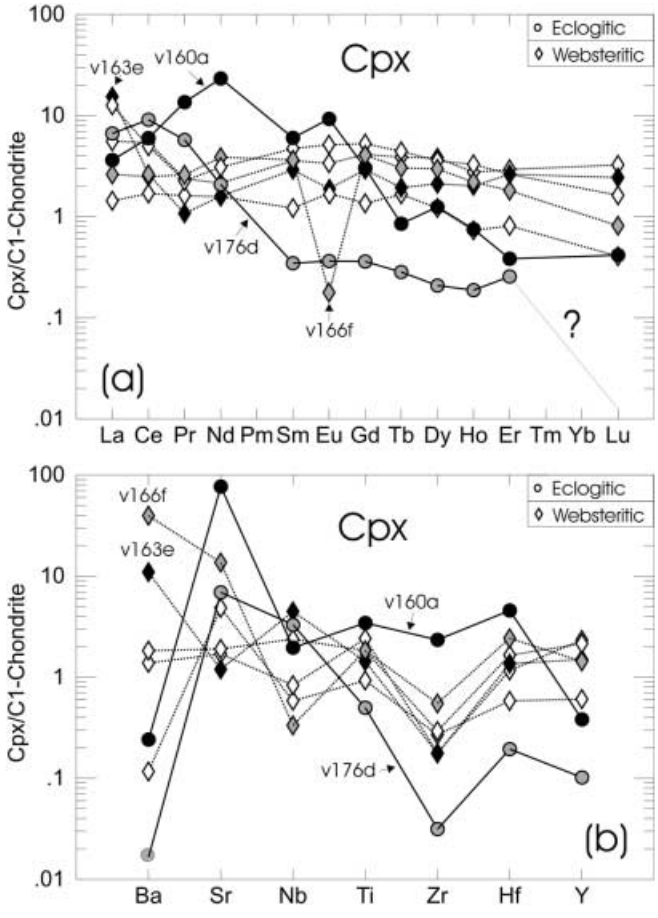

Fig. 4. **a** Clinopyroxene: REE-abundances. Two websteritic inclusions with marked negative Eu anomalies are indicated. **b** LILE and HFSE. Normalised to C1-chondrite of McDonough and Sun (1995)

or ilmenite = 50:50:0; 20:80:0; 80:19:1 and 60:39:1 in order to determine the effect of different mineral modes on trace-element abundances.

Generally, the trace-element abundances of the bulk Venetia eclogite reconstructed from inclusions in diamond v160 plus an assumed Ti-rich phase are very similar for the different modal compositions. They have sub-chondritic Ba concentrations, near chondritic La and Ce concentrations, a positive Sr_N and Eu_N anomaly, negative Hf and Zr anomalies, and two to six times chondritic values from Gd to Y. The differences in the REE abundances are minor, with the assemblage richest in garnet having the highest HREE and lowest LREE. Hf and Zr abundances are marginally higher in the ilmenite-bearing assemblage and lower in the Ti-phase-free bulk rock compared with rutile-bearing eclogite. Nb leaps from two to three times chondritic in ilmenite-bearing or Ti-phase-free assemblages to 40 times chondritic in the rutile-bearing rock. The cpx-poor assemblage has noticeably lower Sr abundances than the other whole-rock reconstructions, reflecting the affinity of Sr for clinopyroxene.

Discussion

Evolution of the eclogitic source

Eclogite genesis is still a highly controversial topic. Many eclogite characteristics, such as the occurrence of 'evolved' phases (SiO_2, K-Feldspar) in the assemblage, stable isotope values and Sr isotopic compositions suggesting hydrothermal alteration or interaction with seawater, and Eu anomalies indicating low-pressure fractionation processes, support models implying crustal protoliths (Ringwood and Green 1967; Helmstaedt et al. 1972; MacGregor and Manton 1986; Shervais et al. 1988; Jacob et al. 1994; Snyder et al. 1997; Jacob and Foley 1999; Barth et al. 2001). A crustal protolith is also implied in experimental and geochemical evidence, which indicates melting of basaltic rocks in the eclogite stability field during subduction and dehydration, which is thought to generate complementary tonalite–trondhjemite–granodiorites (TTGs; Ireland et al. 1994; Rapp and Watson 1995; Winther 1996; Rollinson 1997). On the other hand, a number of workers have produced

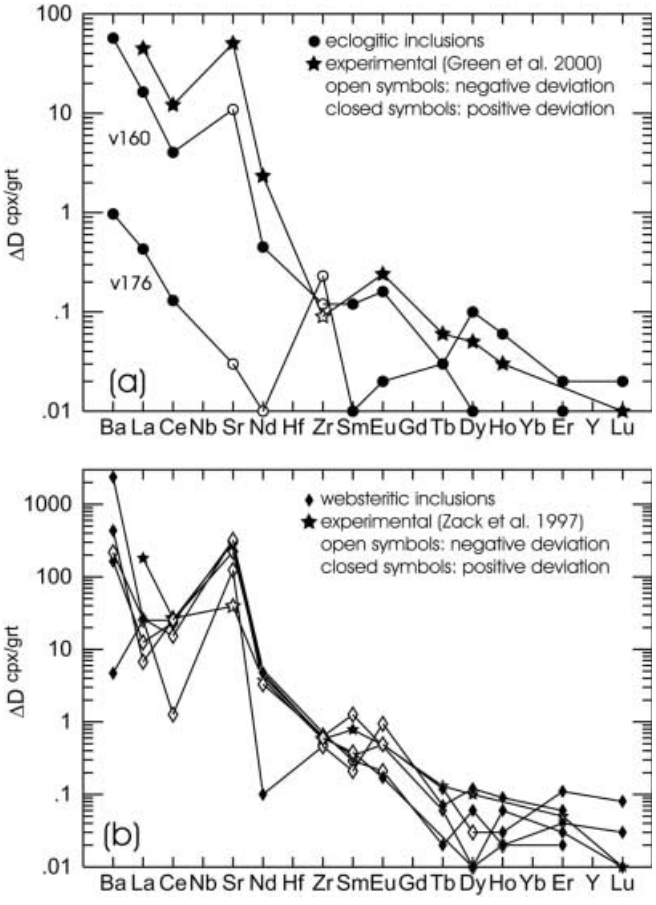

Fig. 5a, b. Deviation of measured from calculated equilibrium clinopyroxene–garnet trace element distribution coefficients (using equation and constants of Harte and Kirkley 1997). **a** Eclogitic diamonds from Venetia and experimental run of Green et al. (2000); **b** websteritic diamonds from Venetia and average garnet pyroxenite xenolith from Kakanui (Zack et al. 1997). *Open symbols* for negative deviation; *closed symbols* for positive deviation. Element order after Hofmann (1988)

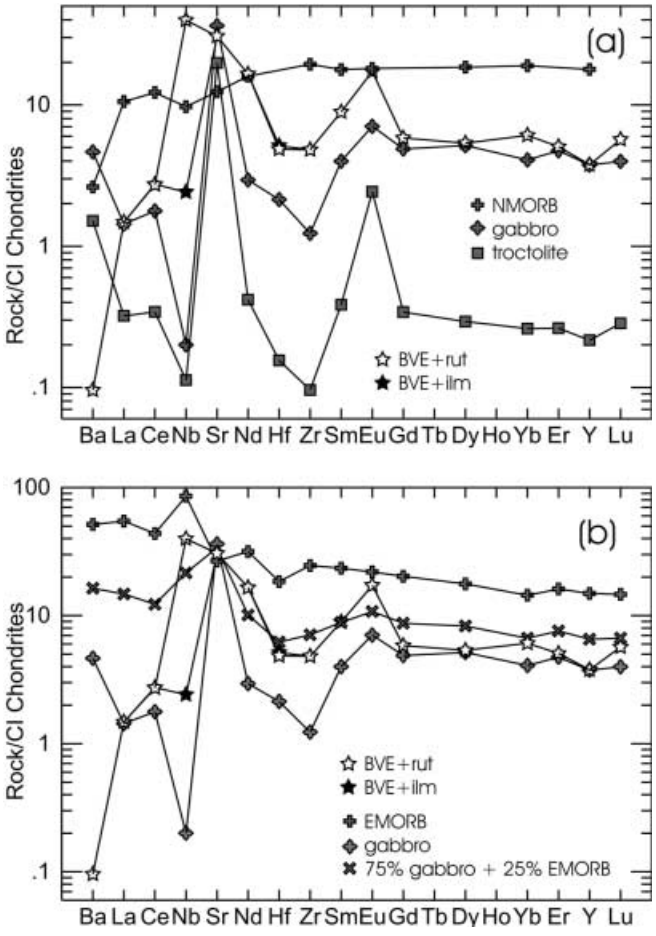

Fig. 6. a NMORB (Sun and McDonough 1989), gabbro and troctolite (Benoit et al. 1996) plotted against the reconstructed bulk eclogite with 60% garnet, 39% cpx plus 1% ilmenite (BVE + ilm) or 1% rutile (BVE + rut), respectively. **b** EMORB (Kamenetsky et al. 1998), gabbro (Benoit et al. 1996) and a mixture of 75% gabbro plus 25% EMORB – to obtain an enriched gabbroic precursor – plotted against BVE + ilm and BVE + rut (see text for details). Normalised to C1-chondrite of McDonough and Sun (1995); element order after Hofmann (1988)

evidence in support of a model of eclogite formation within the mantle, calling on high whole-rock Mg numbers, high Cr and low P contents, mantle-like $\delta^{18}O$ values, garnet and kyanite exsolution from clinopyroxene (believed to be related to cooling from near-solidus temperatures at high pressure) and cumulate textures (Shervais et al. 1988; Smyth et al. 1989; Caporuscio and Smyth 1990; Haggerty et al. 1994; Kopylova et al. 1999). In addition, experiments by Liu and Presnall (2000) indicate that, at 20 kbar, formation of a bi-mineralic garnet–clinopyroxene assemblage in approximately even modal proportions (by fractional crystallisation from a weakly evolved tholeiitic liquid) may indeed be possible. However, at higher pressures (> 30 kbar), olivine is the liquidus phase for melts formed in equilibrium with peridotite, and its primary phase field expands with decreasing pressure (O'Hara and Yoder 1963). This result is in conflict with models that envisage eclogite, an olivine-free assemblage, as high-pressure cumulates of primary peridotite-derived melts.

The observation of positive Eu and Sr anomalies in the reconstructed bulk eclogite at Venetia points toward a low-pressure origin involving a feldspar-enriched cumulate and supports a model involving subducted former oceanic crust. Also, the unfractionated MREE and HREE patterns of the reconstructed whole rock resemble those found in MOR basalts. A crustal origin is in accord with a scenario proposed by Watkeys and Armstrong (1985) for the Limpopo Mobile Belt (into which the Venetia kimberlites intruded), according to which oceanic crust was subducted beneath the central zone in the course of the collision of the Kaapvaal and Zimbabwe cratonic nuclei.

We have taken possible protoliths from mid-ocean ridge settings from the literature and plotted them against reconstructed bulk compositions with 60% garnet, 39% clinopyroxene and 1% rutile or ilmenite, respectively. The relative trace-element abundances of

BVE are most closely mimicked by gabbro (Fig. 6a). However, absolute abundances diverge with regard to HFSE, Ba and the LREE. A significant observation is that none of these rocks shows the negative slope in the REE from Nd to Tb that is displayed by BVE, and which cannot be explained by modal uncertainties. High MREE/HREE may be caused by metasomatic enrichment post-dating formation of the protolith. Alternatively, it could point to a protolith derived from an enriched mantle source, such as a plume-type MORB mantle (Schilling 1975; Sun et al. 1979) or after preferential melting of a clinopyroxene-rich lithology in the source ('marble-cake mantle' Allègre and Turcotte 1986; Kamenetsky et al. 1998; Lassiter et al. 2000).

Assuming that enriched oceanic basalts have gabbroic equivalents and that oceanic rocks in general can show the full range of compositions from purely intrusive to purely extrusive varieties, we calculated a precursor of 75% gabbro plus 25% EMORB. This hypothetical precursor closely approximates the pattern of BVE + ilm, particularly with regard to the slope in REE (Fig. 6b). However, discrepancies for Ba and the LREE persist. These elements would preferentially partition into the melt during partial melting, whereas HREE and Hf, Zr and Nb would be retained in the source if garnet and a Ti-phase are present in the residue. Higher average mantle and slab temperatures during the Archean (Sleep and Windley 1982; Abbott and Hoffman 1984; Martin 1986) may have facilitated slab melting.

To test whether melting of eclogitised MORB-type precursor material reproduces the trace-element pattern of BVE, we modelled the trace-element abundances of residues from different degrees of batch melting (5–30%). Bulk distribution coefficients were calculated (partition coefficients of Green et al. 2000, and Foley et al. 2000) for an eclogite composed of 60% garnet, 39% clinopyroxene and 1% rutile. This corresponds to the modal distribution in the residue of eclogitised basalt produced in melting experiments (Rapp et al. 1999). Not taken into account is a free SiO_2-phase, which should be present in MORB eclogite prior to melting (about 8%, Ryabchikov et al. 1996) and that would be completely stripped out during a partial melting event. The choice of distribution coefficients was guided by our attempt to match pressure, temperature and, in particular, bulk Ca composition as closely as possible to those for BVE. The molar Ca partition coefficient for clinopyroxene–garnet partitioning, with which trace element partition coefficients are strongly correlated (Harte and Kirkley 1997), is 1.61 for BVE and 1.77 for the set of distribution coefficients given for run 1807 in Green et al. (2000).

In a rutile-bearing eclogite precursor the bulk distribution coefficient for Nb is greater than unity; therefore, Nb abundances increase in the residue during partial melting. Melt extraction has virtually no effect on the HREE ($1 < \text{bulk } D < 5$), whereas LREE abundances decrease progressively with increasing cation size (bulk $D \ll 1$). Ba (bulk $D = 0.003$) is even more strongly fractionated into the melt. Despite residual rutile some Zr and Hf is lost to the melt (bulk D 0.228 and 0.152). The compositional range of the residues of different eclogitised oceanic protoliths after extraction of 10% melt is shown in Fig. 7 together with the pattern of BVE + rut.

Our modelling is subject to a number of uncertainties involving parameters such as the composition of the protolith, the pressure and temperature of partial melting and the applicability of partition coefficients. In view of that, the match between BVE + rut and the calculated melting residue of a protolith consisting of 75% gabbro plus 25% EMORB is very good and suggests that ~10% partial melting of a broadly MOR gabbroic precursor rock in the eclogite facies has produced the trace-element abundances exhibited by garnet v160b and clinopyroxene v160a. This conclusion agrees with the finding of Ireland et al. (1994) that partial melting of subducted oceanic crust in the eclogite facies produces residues with a major- and trace-element chemistry similar to eclogitic inclusions in diamond, in particular with regard to $LREE_N$ depletion relative to MORB. Our interpretation is further supported by the calculated whole-rock major element composition of BVE, with MgO, SiO_2 and CaO similar to residues from eclogite melting experiments and to low MgO eclogite xenoliths that have been interpreted as residues of subduction-related partial melting (Barth et al. 2001, and references therein).

Genesis of the garnet websterite source

In studies on mantle xenoliths and on orogenic peridotites, websterites have been identified as discrete dikes, veins or layers, and have been interpreted either as

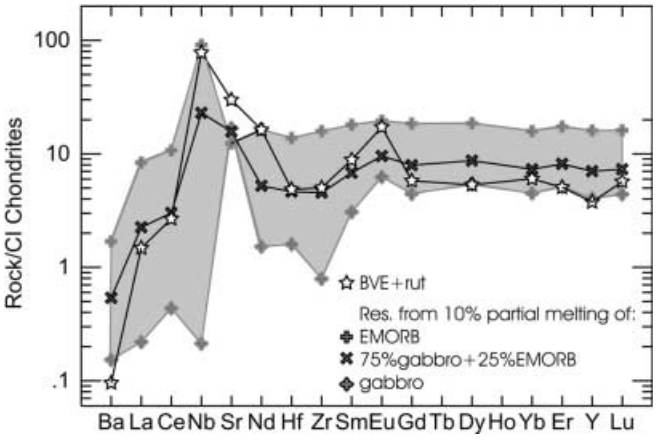

Fig. 7. Range of residues of 10% partial batch melting of eclogitsed gabbro and EMORB and pattern of a mixture of both (75% gabbro and 25% EMORB, references as in Fig. 6), compared with BVE + rut, using a bulk distribution coefficient of 60% garnet, 39% cpx and 1% rutile. Mineral/liquid partition coefficients are from Green et al. (2000, clinopyroxene–/garnet-basaltic melt; $D^{cpx/melt}$ for Sm, Er and Lu are inter- and extrapolated, Ba from Hart and Dunn 1993; $D^{grt/melt}$ for Nb and Ba of Zack et al. 1997) and Foley et al. (2000, rutile–tonalitic melt). Normalised to C1-chondrite of McDonough and Sun (1995); element order after Hofmann (1988)

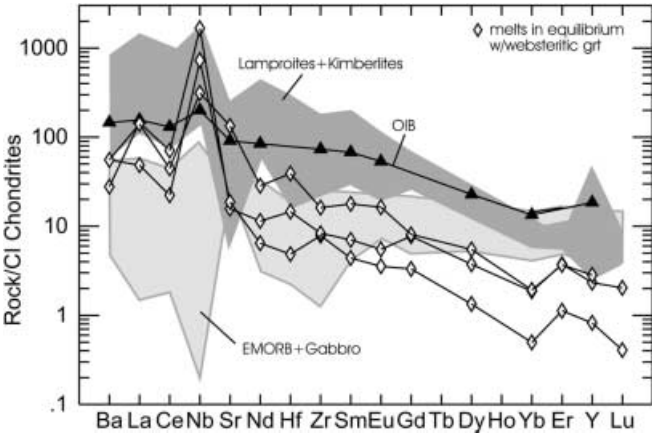

Fig. 8. Ranges of mantle-derived melts from continental and oceanic settings compared with liquids in equilibrium with three websteritic inclusion pairs that show the best fit with the distribution coefficients of Zack et al. (1997). Lamproite melts from Mitchell and Bergmann (1991), kimberlites from Dawson (1980), ocean island basalt from Sun and McDonough (1989), EMORB from Kamenetsky et al. (1998) and gabbro from Benoit et al. (1996). Normalised to C1-chondrite of McDonough and Sun (1995); element order after Hofmann (1988)

remnants of subducted and stretched oceanic crust (Polvé and Allègre 1980; Allègre and Turcotte 1986) or as having crystallised from a melt (e.g. Green and Ringwood 1967). Variations of this igneous model are suggestions that websterites formed as crystal segregates along magma conduits (e.g. Frey and Prinz 1978; Irving 1980; Bodinier et al. 1987; Harte et al. 1987; Litasov et al. 2000) or as cumulates from basaltic melts (e.g. Kornprobst et al. 1990; Nimis and Vannucci 1995). Based on variable oxygen isotopic compositions, radiogenic $^{87}Sr/^{86}Sr$ and Eu anomalies, a recycled crustal component has been postulated for the melt source of some websterites (Pearson et al. 1991, 1993; Becker 1996). In the present data, the positive Eu anomalies in websteritic garnet and clinopyroxene from Venetia exclude direct crystallisation from a melt at high pressure, but would be consistent with a low-pressure protolith accumulating plagioclase. The overall REE patterns of websteritic inclusions, such as low LREE (possibly reflecting a higher fraction of normative orthopyroxene and olivine compared with 'normal' basalt), would be consistent with such an origin. Also, such cumulates have been observed as part of a compositionally heterogeneous oceanic crust. These interpretations have in common that websterites form from primary mantle melts. Although this has been satisfactorily demonstrated for pyroxenite xenoliths from different tectonic settings and peridotite massifs, it may not necessarily apply to websteritic inclusions in diamond.

In order to assess what kind of liquids could have been in equilibrium with the websteritic source, we have calculated the composition of hypothetical melts from websteritic garnet inclusions. We used the distribution coefficients given in Zack et al. (1997), which were determined for pyroxenites with similar $D_{Ca^*}^{cpx/grt}$ to websteritic inclusions from Venetia (Table 3). Melts calculated from websteritic garnets show strong LREE/HREE fractionation, high Nb contents and small positive Eu anomalies. The only exceptions are melts calculated from garnet v199a, which have pronounced La and Nb spikes, and from garnet in the cracked diamond v163. In comparison, high pressure mantle melts, such as kimberlites and melilitites, show a similar degree of REE fractionation, but much higher abundances, whereas oceanic rocks from different sections of oceanic crust show much weaker REE fractionation (Fig. 8). These discrepancies demonstrate that interpretation of the websteritic inclusion paragenesis as a primary mantle melt is unsatisfactory.

Instead, focussing on the intermediate major-element composition of the websteritic paragenesis between eclogite and peridotite, we suggest that the websterite source may be the product of mixing of eclogitic components with mantle peridotite. Such mixing could occur after subduction and melting in the eclogitic portion of the slab and reaction of the melt with overlying peridotite. We would expect the major-element content of the resulting 'mixture' to be transitional between the end members, whereas the trace-element budget, especially for incompatible elements, would be dominated by the invading liquid.

Liquids derived from slab-melting have been experimentally produced and linked to TTG and adakite formation (see above), and they have been invoked for both modal and cryptic metasomatism (Sen and Dunn 1994, and references therein; Yaxley and Green 1998; Rapp et al. 1999, and references therein; Prouteau et al. 2001, and references therein). In those experiments that closely approximate the pressure and temperature of formation of websteritic inclusions (Yaxley and Green 1998; Rapp et al. 1999), the orthopyroxene resulting from a peritectic reaction between peridotitic olivine and melt has a Mg# between 79 and 84. This is similar to websteritic inclusions from Venetia (Mg# = 76–81). Compositional overlap is also observed for TiO_2, Al_2O_3, CaO and Na_2O. Likewise, reacted garnet from these experiments and websteritic garnet inclusions overlap with regard to Cr_2O_3, Mg# and CaO (see also Fig. 1). Websteritic clinopyroxene is compositionally similar to the reacted clinopyroxene of Yaxley and Green, whereas that of Rapp et al. (1999) plots with eclogitic inclusions in diamond (see also Fig. 2).

A mixing origin is difficult to model quantitatively with trace elements because of several unknown factors: (1) the mineral modes of the websteritic end product and the effect of possible later stages of subsolidus re-equilibration or metasomatism, (2) the mineral modes and trace-element abundances of the peridotite that reacts with the slab-derived melts, (3) the composition of the slab and (4) the melt:rock ratio. We can, however, test our hypothesis by comparing the trace-element abundances of 'websteritic melts' with those of silicic slab-derived melts. Rapp et al. (1999) investigated the reaction between such melts and peridotite and determined

the trace-element composition of melts derived directly from eclogitised basalt and those that assimilated various amounts of peridotite. A comparison of these compositions with our 'websteritic melts' shows some similarity in slope (Fig. 9, inset), but concentrations of most elements are more than an order of magnitude higher in the experimental melts, and they have negative Nb spikes.

We also calculated a hypothetical melt by applying the enrichment factor given by Rapp et al. (1999, to calculate a 30% partial melt of any eclogitised basaltic composition) to EMORB, gabbro and the hypothetical protolith of BVE (75% MOR gabbro + 25% EMORB, see eclogite discussion above). Involving this assumed eclogite precursor with its trace element characteristics in the modelling results in a much improved fit with the 'websteritic melts' with regard to both absolute and relative abundances, despite uncertainties in the exact nature of the protolith and the melting (Fig. 9). Nb is again an exception, but this may be partially attributed to the fact that the enrichment factor of Rapp et al. (1999) was obtained with 1% residual rutile in the source, which would effectively retain Nb (bulk $D = 2.59$), resulting in low Nb concentrations in the melt. Small degrees of melting in the absence of a residual Ti phase decreases D_{Nb} to 0.004 and would lead to a significant increase in Nb_N in the melt. Small degrees of melting could also explain the enrichment of the highly incompatible element Ba observed in websteritic clinopyroxene, which is not observed for eclogitic clinopyroxene.

The experimental evidence matches our mixing model both with regard to major- and trace-element concentrations. This model is also consistent with variable $\delta^{18}O$ and radiogenic initial Os and Sr isotopic compositions in some websterite xenoliths, which require input of a component with long-term evolution in a high Re/Os and Rb/Sr environment (e.g. Pearson et al. 1991, 1993). Mantle-derived melts, such as basalts, fit this requirement. Based on trace-element and isotopic evidence, Pearson et al. (1991, 1993) suggested that websterites from the Beni Bousera peridotite massif, North Morocco, were derived directly from melts of various sections of oceanic crust fractionating garnet and two pyroxenes. However, cumulates from melts should not be more refractory than the source region of the melt. In contrast, websteritic inclusions in diamond are chemically more depleted than eclogitic minerals. Therefore, we consider crustal trace-element and isotope signatures in websterites as inherited from a slab-derived melt that reacted with surrounding peridotite. The REE patterns of some of the websteritic inclusions in diamond from Venetia indicate an additional LREE enrichment event, and this metasomatic pulse may have triggered diamond growth in the websteritic environment.

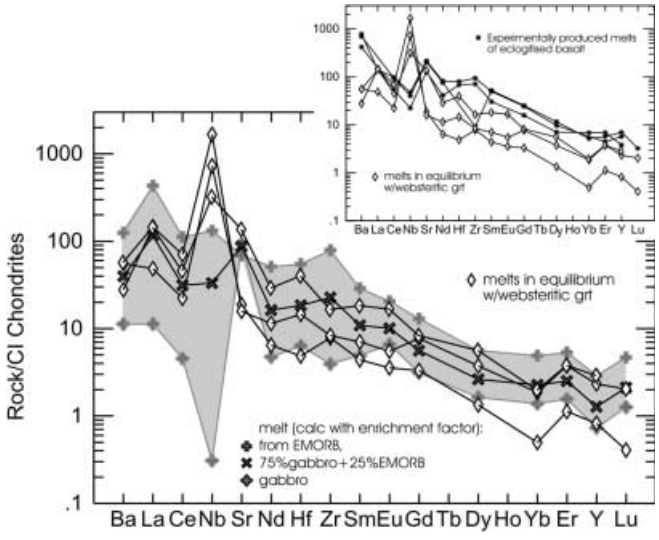

Fig. 9. Comparison of melts in equilibrium with three websteritic garnets with the range of melts calculated by applying the enrichment factor of Rapp et al. (1999, for calculation of 30% partial melt of any eclogitised basalt) to gabbro and EMORB, and to an assumed enriched gabbroic precursor (mixture of 75% gabbro, plus 25% EMORB). *Inset* shows melts of eclogitised basalt produced in experiments of Rapp et al. (1999). Nb contents in the calculated slab melts are small because of the high degree of partial melting and residual rutile in the experiments from which the enrichment factor was determined. At small melting degrees and in the absence of rutile in the residue, Nb contents in the melt could become much larger. Normalised to C1-chondrite of McDonough and Sun (1995); element order after Hofmann (1988)

Conclusions

Reconstruction of an eclogitic bulk rock composition from garnet and clinopyroxene inclusions coexisting in a diamond from Venetia reveals characteristics (depleted $LREE_N$, enriched and flat $MREE_N$–$HREE_N$, positive Eu and Sr anomalies) indicative of a protolith representing subducted oceanic crust: flat $MREE_N$–$HREE_N$ imply that the magmatic precursor crystallised from a melt derived from above the garnet stability field, whereas positive Eu and Sr anomalies point to accumulation of plagioclase. Depletion in Ba and LREE, relative to oceanic crust, can be modelled by extraction of ~10% partial melt after eclogitisation of an enriched gabbroic precursor. This enrichment may be inherited from the MORB source or be a result of later metasomatism. The combination of these processes can reproduce the absolute and relative trace-element abundances of the reconstructed bulk eclogite.

Eu anomalies in some websteritic garnet and clinopyroxene inclusions from Venetia imply a component that experienced feldspar fractionation, which again points towards a contribution of subducted oceanic crust, thus establishing a link between eclogitic and websteritic diamond sources. Recent experimental work (Yaxley and Green 1998; Rapp et al. 1999; Prouteau et al. 2001) has simulated the infiltration of peridotite by silicic and incompatible element-rich partial melts of eclogite. These impregnated peridotites have major

element compositions that overlap with those of websteritic inclusions in diamond. We propose that the websteritic source at Venetia is the product of a reaction between slab-derived melts and peridotitic lithospheric mantle resulting in the observed intermediate major element composition and a trace-element budget dominated by the percolating melt. In support of that, our modelling shows that low volume melts derived from the eclogitic portion of a subducting slab match the trace element composition of melts in equilibrium with websteritic garnet inclusions.

Acknowledgements We are grateful to John Craven at Edinburgh University for his help with the ion microprobe. Trevor Green is thanked for helpful discussions on trace-element partitioning. Thorough and constructive reviews by B. Harte, D. Jacob, L.A. Taylor and R. Vannucci greatly improved the manuscript. Funding by the Deutsche Forschungsgemeinschaft (DFG) and additional support through DeBeers Consolidated Mines Ltd are gratefully acknowledged. This is publication no 260 in the GEMOC National Key centre.

References

Abbott DH, Hoffman SE (1984) Archean plate tectonics revisited 1. Heat flow, spreading rate, and the age of subducting oceanic lithosphere and their effects on the origin and evolution of continents. Tectonics 3:429–448

Allègre CJ, Turcotte DL (1986) Implications of a two-component marble-cake mantle. Nature 323:123–127

Barth MG, Rudnick RL, Horn I, McDonough WF, Spicuzza MJ, Valley JW, Haggerty SE (2001) Geochemistry of xenolithic eclogites from West Africa, Part I: a link between low MgO eclogites and Archean crust formation. Geochim Cosmochim Acta 65:1499–1527

Becker H (1996) Crustal trace element and isotopic signatures in garnet pyroxenites from garnet peridotite massifs from lower Austria. J Petrol 4:785–810

Benoit M, Polvé M, Ceuleneer G (1996) Trace element and isotopic characterization of mafic cumulates in a fossil mantle diapir (Oman ophiolite). Chem Geol 134:199–214

Bodinier J-L, Guiraud M, Fabriès J, Dostal J, Dupuy C (1987) Petrogenesis of layered pyroxenites from the Lherz, Freychinède and Prades ultramafic bodies (Ariège, French Pyrenées). Geochim Cosmochim Acta 51:279–290

Caporuscio FA, Smyth JR (1990) Trace element crystal chemistry of mantle eclogites. Contrib Mineral Petrol 105:550–561

Dawson JB (1980) Kimberlites and their xenoliths. Springer, Berlin Heidelberg New York

Deines P, Harris JW, Gurney JJ (1993) Depth-related carbon isotope and nitrogen concentration variability in the mantle below the Orapa kimberlite, Botswana, Africa. Geochim Cosmochim Acta 57:2781–2796

Foley SF, Barth MG, Jenner GA (2000) Rutile/melt partition coefficients for trace elements and an assessment of the influence of rutile on the trace element characteristics of subduction zone magmas. Geochim Cosmochim Acta 64:933–938

Frey FA, Prinz M (1978) Ultramafic inclusions from San Carlos, Arizona: petrologic and geochemical data bearing on their petrogenesis. Earth Planet Sci Lett 38:129–176

Fujimaki H, Tatsumoto M, Aoki K (1984) Partition coefficients of Hf, Zr, and REE between phenocrysts and groundmasses. J Geophys Res Suppl 89:B662–B672

Green DH, Ringwood AE (1967) The genesis of basaltic magmas. Contrib Mineral Petrol 15:103–190

Green TH, Blundy JD, Adam J, Yaxley GM (2000) SIMS determination of trace element partition coefficients between garnet, clinopyroxene and hydrous basaltic liquids at 2–7.5 GPa and 1,080–1,200 °C. Lithos 53:165–187

Gurney JJ (1984) A correlation between garnets and diamonds in kimberlites. In: Glover JE, Harris PG (eds) Kimberlite occurrence and origin: a basis for conceptual models in exploration, vol 8. Publishers of the Geology Department and University Extension, University of Western Australia, pp 143–166

Gurney JJ, Harris JW, Rickard RS (1984) Silicate and oxide inclusions in diamonds from the Orapa Mine, Botswana. In: Kornprobst J (ed) Kimberlites II: the mantle and crust–mantle relationships. Elsevier, Amsterdam, pp 1–9

Haggerty SE, Fung AT, Burt DM (1994) Apatite, phosphorus and titanium in eclogitic garnet from the upper mantle. Geophys Res Lett 21:1699–1702

Hart SR, Dunn T (1993) Experimental cpx/melt partitioning of 24 trace elements. Contrib Mineral Petrol 113:1–8

Harte B, Kirkley MB (1997) Partitioning between clinopyroxene and garnet: data from mantle eclogites. Chem Geol 136:1–24

Harte B, Winterburn, PA, Gurney JJ (1987) Metasomatic and enrichment phenomena in garnet peridotite facies mantle xenoliths from the Matsoku kimberlite pipe, Lesotho. In: Menzies MA, Hawkesworth CJ (eds) Mantle metasomatism. Academic Press, New York, pp 145–220

Helmstaedt H, Anderson OL, Gavasci AT (1972) Petrofabric studies in eclogite, spinel websterite, and spinel lherzolite xenoliths from kimberlite-bearing breccia pipes in southeastern Utah and northeastern Arizona. J Geophys Res 77:4350–4365

Hofmann AW (1988) Chemical differentiation of the Earth: the relationship between mantle, continental crust, and oceanic crust. Earth Planet Sci Lett 90:297–314

Ireland TR, Rudnick RL, Spetsius Z (1994) Trace elements in diamond inclusions from eclogites reveal link to Archean granites. Earth Planet Sci Lett 128:199–213

Irving J (1980) Petrology and geochemistry of composite ultramafic xenoliths in alkalic basalts and implications for magmatic processes within the mantle. Am J Sci 280A:389–426

Jacob DE, Foley SF (1999) Evidence for Archean ocean crust with low high field strength element signature from diamondiferous eclogite xenoliths. Lithos 48:317–336

Jacob D, Jagoutz E, Lowry D, Mattey D, Kudrjavtseva G (1994) Diamondiferous eclogites from Siberia: remnants of Archean oceanic crust. Geochim Cosmochim Acta 58:5191–5207

Kamenetsky VS, Eggins SM, Crawford AJ, Green DH, Gasparon M, Falloon TJ (1998) Calcic melt inclusions in primitive olivine at 43° N MAR: evidence for melt-rock reaction/melting involving clinopyroxene-rich lithologies during MORB generation. Earth Planet Sci Lett 160:115–132

Keller RA, Taylor LA, Snyder GA, Sobolev VN, Carlson WD, Sobolev NV (1999) Detailed pull-apart of a diamondiferous eclogite xenolith: Implications for mantle processes during diamond genesis, vol 1. Proc 7th Int Kimberlite Conference, Red Roof Design, Cape Town, pp 397–412

Kopylova MG, Russell JK, Cookenboo H (1999) Petrology of peridotite and pyroxenite xenoliths from the Jericho kimberlite: implications for the thermal state of the mantle beneath the Slave Craton, northern Canada. J Petrol 40:79–104

Kornprobst J, Piboule M, Roden M, Tabit A (1990) Corundum-bearing garnet clinopyroxenites at Beni Bousera (Morocco): original plagioclase-rich gabbros recrystallised at depth within the mantle? J Petrol 31:717–745

Lassiter JC, Hauri EH, Reiners PW, Garcie MO (2000) Generation of Hawaiian post-erosional lavas by melting of a mixed lherzolite/pyroxenite source. Earth Planet Sci Lett 178:269–284

Litasov KD, Foley SF, Litasov YD (2000) Magmatic modification and metasomatism of the subcontinental mantle beneath the Vitim volcanic field (east Siberia): evidence from trace element data on pyroxenite and peridotite xenoliths from Miocene picrobasalt. Lithos 54:83–114

Liu T-C, Presnall DC (2000) Liquidus phase relations in the system $CaO–MgO–Al_2O_3–SiO_2$ at 2.0 GPa: applications to basalt fractionation, eclogites, and igneous sapphirine. J Petrol 41: 3–20

MacGregor ID, Manton WI (1986) Roberts Victor eclogites: ancient oceanic crust. J Geophys Res 91:14093–14079
Martin H (1986) Effect of steeper Archean geothermal gradient on geochemistry of subduction zone magmas. Geology 14:753–756
McDonough WF, Sun SS (1995) The composition of the Earth. Chem Geol 120:223–253
Meyer HOA (1987) Inclusions in diamond. In: Nixon PH (ed) Mantle xenoliths. Wiley, Chichester, pp 501–522
Meyer HOA, Boyd FR (1972) Composition and origin of crystalline inclusions in natural diamonds. Geochim Cosmochim Acta 36:1255–1273
Mitchell RH, Bergmann SC (1991) Petrology of lamproites. Plenum Press, New York
Nielsen RL, Gallahan WE, Newberger F (1992) Experimentally determined mineral-melt partition coefficients for Sc, Y and REE for olivine, orthopyroxene, pigeonite, magnetite and ilmenite. Contrib Mineral Petrol 110:488–499
Nimis P, Vannucci R (1995) An ion microprobe study of clinopyroxenes in websteritic and megacrystic xenoliths from Hyblean Plateau (SE Sicily, Italy) – constraints of HFSE/REE/Sr fractionation at mantle depth. Chem Geol 124:185–197
O'Hara MJ, Yoder HS Jr (1963) Partial melting of the mantle. Carnegie Inst Wash Yearbook 62:66–71
Paster DP, Schauwecker DS (1974) The behaviour of some trace elements during solidification of the Skaergaard layered series. Geochim Cosmochim Acta 38:1549–1577
Pearson DG, Davies GR, Nixon PH, Greenwood PB, Mattey DP (1991) Oxygen isotope evidence for the origin of pyroxenites in the Beni Bousera peridotite massif, North Morocco: derivation from subducted oceanic lithosphere. Earth Planet Sci Lett 102:289–301
Pearson DG, Davies GR, Nixon PH (1993) Geochemical constraints on the petrogenesis of diamond facies pyroxenites from the Beni Bousera peridotite massif, North Morocco. J Petrol 35:1–48
Polvé M, Allègre CJ (1980) Orogenic lherzolite complexes studied by ^{87}Rb–^{87}Sr: a clue to understand the mantle convection process. Earth Planet Sci Lett 51:71–93
Prouteau G, Scaillet B, Pichavant M, Maury R (2001) Evidence for mantle metasomatism by hydrous silicic melts derived from subducted oceanic crust. Nature 410:197–200
Rapp RP, Watson EB (1995) Dehydration melting of metabasalt at 8–32 kbar: implications for continental growth and crust–mantle recycling. J Petrol 36:891–931
Rapp RP, Shimizu N, Norman MD, Applegate GS (1999) Reaction between slab-derived melts and peridotite in the mantle wedge: experimental constraints at 3.8 GPa. Chem Geol 160:335–356
Ringwood AE, Green DH (1967) An experimental investigation of the gabbro-eclogite transformation and some geophysical implications. Tectonophysics 3:383–427
Rollinson H (1997) Eclogite xenoliths in west African kimberlites as residues from Archaean granitoid crust formation. Nature 389:173–176
Rudnick RL, Barth M, Horn I, McDonough WF (2000) Rutile-bearing refractory eclogites: missing link between continents and depleted mantle. Science 287:278–281
Ryabchikov ID, Miller C, Mirwald PW (1996) Composition of hydrous melts in equilibrium with quartz eclogites. Mineral Petrol 58:101–110
Ryerson FJ, Watson, EB (1987) Rutile saturation in magmas: implications for Ti–Nb–Ta depletion in island-arc basalts. Earth Planet Sci Lett 86:225–239
Sassi R, Harte B, Carswell DA, Yujing H (2000) Trace element distribution in Central Dabie eclogites. Contrib Mineral Petrol 139:298–315
Schilling JG (1975) Rare-earth variations across 'normal segments' of the Reykjanes Ridge, 60–53°N, Mid-Atlantic Ridge, 29°S, and East Pacific Rise, 2–19°S, and evidence of the composition of the underlying low-velocity layer. J Geophys Res 80:1459–1473
Sen C, Dunn T (1994) Dehydration melting of a basaltic composition amphibolite at 1.5 and 2.0 GPa: implications for the origin of adakites. Contrib Mineral Petrol 117:394–409
Shervais JW, Taylor LA, Lugmair GW, Clayton RN, Mayeda TK, Korotev RL (1988) Early Proterozoic oceanic crust and the evolution of subcontinental mantle: eclogites and related rocks from southern Africa. Geol Soc Am Bull 100:411–423
Sleep NH, Windley BF (1982) Archaean plate tectonics: constraints and inferences. J Geol 90:363–379
Smyth JR, Caporuscio FA, McCormick TC (1989) Mantle eclogites, Udachnaya kimberlite pipe, Yakutia, Siberia: evidence of differentiation in the early Earth? Earth Planet Sci Lett 93:133–141
Snyder GA, Taylor LA, Crozaz G, Halliday AN, Beard BL, Sobolev VN, Sobolev NV (1997) The origins of Yakutian eclogite xenoliths. J Petrol 38:85–113
Sobolev NV (1977) Deep-seated inclusions in kimberlites and the problem of the composition of the upper mantle (translated from the Russian edn, 1974). Am Geophys Union, Washington
Sobolev NV, Lavrent'ev YG, Pokhilenko NP, Usova LV (1973) Chrome-rich garnets from the kimberlites of Yakutia and their paragenesis. Contrib Mineral Petrol 40:39–52
Sobolev NV, Kaminsky FV, Griffin WL, Yefimova ES, Win TT, Ryan CG, Botkunov AI (1997) Mineral inclusions in diamonds from the Sputnik kimberlite pipe, Yakutia. Lithos 39:135–157
Sobolev NV, Snyder GA, Taylor LA, Keller RA, Yefimova ES, Sobolev VN, Shimizu N (1998) Extreme chemical diversity in the mantle during eclogitic diamond formation: evidence from 35 garnet and 5 pyroxene inclusions in a single diamond. Int Geol Rev 40:567–578
Stachel T, Harris JW (1997) Syngenetic inclusions in diamond from the Birim field (Ghana) – a deep peridotitic profile with a history of depletion and re-enrichment. Contrib Mineral Petrol 127:336–352
Stachel T, Harris JW, Brey GP (1998) Rare and unusual mineral inclusions in diamonds from Mwadui, Tanzania. Contrib Mineral Petrol 132:34–47
Stachel T, Harris JW, Brey GP (1999) REE patterns of peridotitic and eclogitic inclusions in diamonds from Mwadui (Tanzania), vol 2. Proc 7th Int Kimberlite Conf, Red Roof Design, Cape Town, pp 829–835
Sun SS, McDonough WF (1989) Chemical and isotopic systematics of oceanic basalts: implications for mantle composition and processes. In: Saunders AD, Norry MJ (eds) Magmatism in the ocean basins. Geol Soc Lond Spec Publ 42:313–345
Sun SS, Nesbitt RW, Sharaskin AY (1979) Geochemical characteristics of mid-ocean ridge basalts. Earth Planet Sci Lett 44:119–138
Taylor LA, Snyder GA, Crozaz G, Sobolev VN, Yefimova ES, Sobolev NV (1996) Eclogitic inclusions in diamonds: evidence of complex mantle processes over time. Earth Planet Sci Lett 142:535–551
Taylor LA, Milledge HJ, Bulanova CP, Snyder GA, Keller RA (1998) Metasomatic eclogitic diamond growth: evidence from multiple diamond inclusions. Int Geol Rev 40:592–604
Taylor LA, Keller RA, Snyder GA, Wang W, Carlson WD, Hauri EH, McCandless T, Kim K-R, Sobolev NV, Bezborodov SM (2000) Diamonds are their mineral inclusions, and what they tell us: a detailed 'pull-apart' of a diamondiferous eclogite. Int Geol Rev 42:959–983
Viljoen KS, Phillips D, Harris JW, Robinson DN (1999) Mineral inclusions in diamonds from the Venetia Kimberlites, northern Province, South Africa, vol 2. Proc 7th Int Kimberlite Conf, Red Roof Design, Cape Town, pp 888–895
Watkeys MK, Armstrong RA (1985) The importance of being alkaline – deformed Late Archaean lamprophyric dykes, Central Zone, Limpopo Belt. Trans Geol Soc S Afr 88:195–206
Winther KT (1996) An experimentally based model for the origin of tonalitic and trondhjemitic melts. Chem Geol 127:43–59
Yaxley GM, Green DH (1998) Reactions between eclogite and peridotite: mantle refertilisation by subduction of oceanic crust. Schweiz Mineral Petrogr Mitt 78:243–255
Zack T, Foley SF, Jenner GA (1997) A consistent partition coefficient set for cpx, amphibole and garnet from laser ablation microprobe analysis of garnet pyroxenites from Kakanui, New Zealand. Neues Jahrb Miner Abh 172:23–41